Optimization-Based Scheduling of Grid-Scale Li-Ion Battery Energy Storage System for Participation in Japan's FCR Market

Hossam Ashraf[1], Sinan Cai[1], Masahiro Mae[1], Ryuji Matsuhashi[1]

[1] The University of Tokyo, 7-3-1 Hongo, Bunkyo-ku, 113-8656, Tokyo, Japan,
{hossam,cai,mae,matu}@enesys.t.u-tokyo.ac.jp

***Abstract*— Grid-scale battery energy storage systems (BESS) are increasingly expected to deliver both energy arbitrage and frequency containment reserve (FCR) services. Accordingly, this paper presents a market-compliant optimization framework to assess large-scale BESS operation in Japan. Explicitly, the model enforces FCR Assessment-I while accounting for thermal behavior and degradation. Using real market, load, and environmental data over a continuous six-month horizon, four participation scenarios are evaluated. Results show that energy arbitrage-only reduces net cost by approximately 25% compared to baseline operation but induces severe cycling and degradation. In contrast, FCR participation fundamentally reshapes performance. Economically, capacity revenues yield over 700% improvement in net economic outcome relative to non-FCR cases. Simultaneously, daily state-of-charge swings decrease by more than 50%, while degradation remains tightly bounded. Thus, these results demonstrate that reserve-oriented dispatch enables both high profitability and physically sustainable BESS operation.**

***Index Terms*-- Battery Energy Storage System, Degradation Cost, Frequency Containment Reserve, Thermal Management.**

I. INTRODUCTION

Ongoing deregulation, increasing renewable penetration, and declining system inertia are placing growing demands on frequency stability in modern power systems. Consequently, In Japan, these trends have heightened the need for fast and flexible balancing resources capable of responding to short-term frequency deviations under market-based operation. Particularly, recent system-level studies emphasize that distributed flexibility resources will be essential for maintaining secure and resilient operation in future Japanese power systems [1]. Among available technologies, battery energy storage systems (BESSs) are particularly well suited for frequency containment reserve (FCR) services due to their rapid response and bidirectional power capability.

Accordingly, several studies have examined BESS operation in the Japanese electricity market, focusing mainly on economic dispatch using Japan electric power exchange (JEPX) price signals [2], local energy management and imbalance compensation [3], and resilience enhancement through battery-PV coordination [4]. In addition, recent reports identify ancillary service provision as a key opportunity for grid-scale battery deployment in Japan [5]. However, these works primarily address energy arbitrage or local objectives and do not explicitly model participation in the Japanese FCR market under realistic reserve requirements and assessment rules.

On the other side, internationally, BESS participation in frequency regulation markets has been studied in greater detail. For example, the authors in [6], [7] demonstrated the importance of accounting for operational constraints and degradation effects when evaluating feasibility and profitability. Nevertheless, the market structures and assessment procedures considered in these studies differ significantly from those applied in Japan, limiting the direct applicability of their conclusions.

To address this gap, this paper proposes a market-compliant mixed integer linear programing (MILP) framework for large-scale BESS participation in Japan's FCR market. In contrast to prior studies, the formulation explicitly enforces Assessment I compliance, bid deliverability, and market rules within the optimization. Furthermore, thermal dynamics and degradation costs are also embedded, enabling realistic evaluation of high-utilization operation using actual Japanese spot and FCR price data. Hence, the main contributions are threefold:

C1) A unified scheduling framework that enforces Japan's FCR Assessment I requirements end-to-end, closing the gap between optimized bids and qualification feasibility,

C2) a quantitative assessment of how energy export and FCR participation reshape dispatch behavior, SoC trajectories, and reserve headroom, and

C3) demonstration that explicitly modeling thermal and degradation constraints materially alters reserve feasibility and economic outcomes compared to simplified BESS models.

979-8-3195-3554-2/26/$31.00 ©2026 IEEE

II. SYSTEM MODEL AND MARKET COUPLING

The study considers a grid-connected BESS coupled to Japan's spot energy and FCR markets, as illustrated in Fig. 1. The BESS exchanges power with the grid at the point of common coupling (PCC), purchasing energy for charging or exporting energy during discharging at JEPX spot prices. In parallel, the BESS may provide FCR by reserving symmetric upward and downward capacity and receiving capacity payments independent of activation energy.

Practically, battery operation determines the state of charge and supplies both exported power and a non-dispatchable electric vehicle (EV) charging demand within the scope of this study. In addition, a heat, ventilation, and air conditioning (HVAC) system draws electrical power from the PCC to maintain battery temperature within prescribed limits.

Exclusively, this work focuses on FCR Assessment I. Although Assessment I permits reserve shortfalls with penalties, reserve deliverability is enforced here as a hard constraint. Consequently, all committed FCR capacity must remain physically deliverable considering battery operation, EV demand, and auxiliary power consumption.

III. OPTIMIZATION PROBLEM FORMULATION

The BESS scheduling problem is formulated as an MILP model over discrete time steps $t \in \mathcal{T} = 8832$ and FCR market blocks $b \in \mathcal{B} = 1472$. Specifically, the formulation jointly optimizes energy trading, reserve provision, thermal operation, and degradation-aware scheduling under Japanese FCR rules.

A. Objective Function

Principally, the optimization seeks to minimize the total operating cost by accounting for energy purchases, reserve revenues, energy exports, and battery degradation, as described by (1).

$$\min J = \sum_{t\in\mathcal{T}} p_t^{buy}\left(\frac{P_t^{ch}}{\eta_{ch}} + P_t^{HVAC}\right)\Delta t - \sum_{b\in\mathcal{B}} Q_b\, p_b^{FCR} T_b - \sum_{t\in\mathcal{T}} p_t^{sell} P_t^{exp}\Delta t + \sum_{t\in\mathcal{T}} C_{deg}\,\Delta t \qquad (1)$$

where, p_t^{buy} and p_t^{sell} are the spot purchase and selling prices at time t [JPY/kWh], respectively. P_t^{ch} and P_t^{HVAC} denote the battery charging power and HVAC electric power [MW], respectively. The charging efficiency is symbolized by η_{ch}. Δt is the slot duration [0.5 h], Q_b is the symmetric FCR capacity reserved in block b [MW], p_b^{FCR} is the FCR capacity price [JPY/kW/0.5h], and T_b is the duration of block b [3 h]. Finally, P_t^{exp} is the exported power and C_{deg} represents the BESS degradation cost at time t [JPY].

B. Electrical and Energy Constraints

To represent feasible battery operation, charging and discharging powers are limited by rated capacity and mutually exclusive operation, as shown in (2)-(4).

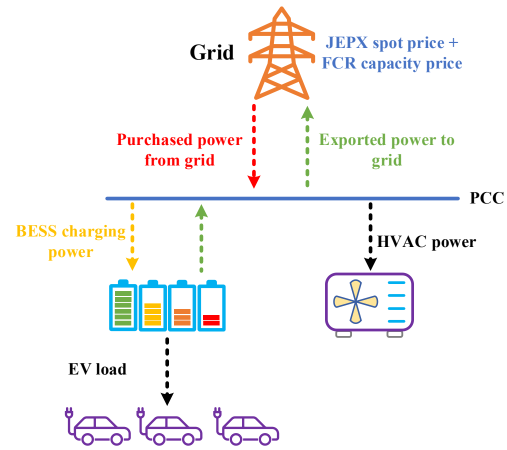

Fig. 1. System and market coupling for BESS participation in the Japanese FCR market

$$0 \le P_t^{ch} \le U_t^{ch} P_{rated} \qquad (2)$$

$$0 \le P_t^{dis} \le U_t^{dis} P_{rated} \qquad (3)$$

$$U_t^{ch} + U_t^{dis} \le 1 \qquad (4)$$

where, P_t^{dis} defines the battery discharging power [MW], P_{rated} is the rated power capacity of the BESS [MW], and U_t^{ch} and $U_t^{dis} \in \{0,1\}$ are binary variables preventing simultaneous charging and discharging.

Furthermore, given these power decisions, the battery state of charge (SoC) evolves according to energy conservation, as given by (5) [8]. Moreover, to ensure physically admissible operation and avoid end-effects, SoC limits and a terminal constraint are enforced, as expressed in (6).

$$E_{t+1} = E_t + \eta_{ch} P_t^{ch}\Delta t - \frac{1}{\eta_{dis}} P_t^{dis}\Delta t \qquad (5)$$

$$E_{min} \le E_t \le E_{max}, \quad E_\infty = E_0 \qquad (6)$$

where, E_t is the battery energy at time t [MWh], η_{dis} is the discharging efficiency, E_{min} and E_{max} are the BESS's SoC limits [MWh], and E_0 and E_∞ denote initial and terminal SoC [MWh].

In addition to market participation, the BESS must supply a non-dispatchable EV demand, as formulated by (7).

$$P_t^{srv} = D_t^{EV} \qquad (7)$$

where, P_t^{srv} is power supplied to EV charging [MW] and D_t^{EV} is the fixed EV load profile [MW].

Finally, the net power exported to the grid is then determined by battery discharge after serving the EV load, as in (8).

$$P_t^{exp} = \eta_{dis} P_t^{dis} - P_t^{srv} \qquad (8)$$

C. FCR Participation Constraints

FCR participation is modeled by reserving symmetric capacity subject to market limits and bid granularity, as formulated in (9)-(11).

$$Q_{min} \leq Q_b \leq Q_{max} \quad (9)$$

$$Q_b = n_b . y_b \quad (10)$$

$$y_b \epsilon \{0,1\} \quad (11)$$

where, Q_{max} are Q_{min} the maximum and minimum allowable bidding capacity [MW]. n_b is an integer granularity variable reflecting the minimum bid increment [kW], and y_b is a binary variable indicating whether an FCR bid is placed in block b.

To ensure Assessment I compliance, the reserved FCR capacity must remain deliverable given the available energy throughout the block, as constrained by (12) and (13).

$$Q_{b(t)} \leq \frac{\eta_{dis}}{h_t^{rem}} (E_t - E_{min}) \quad (12)$$

$$Q_{b(t)} \leq \frac{E_{max} - E_t}{\eta_{ch} h_t^{rem}} \quad (13)$$

where, h_t^{rem} is the remaining duration of the FCR block [h].

D. Thermal System Constraints

To capture the coupling between electrical operation and temperature evolution, battery thermal dynamics are modeled using a lumped energy balance, as expressed by (14) [9].

$$C_{th} \frac{T_{t+1}^b - T_t^b}{\Delta t} = q_t^{gen} + UA(T_{amb}^t - T_t^b) - q_t^{cool} - q_t^{heat} \quad (14)$$

where, T_t^b is battery temperature [°C], T_{amb}^t is ambient temperature [°C], C_{th} is thermal capacitance [MWh/°C], and UA is thermal conductance [MW/°C]. q_t^{gen}, q_t^{cool}, and q_t^{heat} represent the internal heat generation, and the corresponding cooling and heating thermal outputs [MW_{th}], respectively.

Additionally, for a safe operation, hard temperature bounds are imposed by (15).

$$T_{min} \leq T_t^b \leq T_{max} \quad (15)$$

On the other side, q_t^{gen} is linked directly to charging and discharging losses, as depicted in (16).

$$q_t^{gen} = \left(\frac{1}{\eta_{dis}} - 1\right) P_t^{dis} + (1 - \eta_{ch}) P_t^{ch} \quad (16)$$

Accordingly, the electrical power consumed by the HVAC system is bounded and directly coupled to the heating and cooling thermal outputs through fixed coefficients of performance, as expressed by (17)-(19).

$$0 \leq P_t^{cool} + P_t^{heat} \leq P_{max}^{HVC} \quad (17)$$

$$q_t^{heat} \leq COP_h P_t^{heat} \quad (18)$$

$$q_t^{cool} \leq COP_c P_t^{cool} \quad (19)$$

where, P_t^{cool} and P_t^{heat} denote the electrical power consumed by the cooling and heating units [MW], respectively. P_{max}^{HVC} is the maximum available HVAC electrical capacity [MW]. COP_c and COP_h represent the coefficients of performance of the cooling and heating systems, respectively.

E. Degradation Model

Lastly, to internalize aging effects, battery degradation is represented using a piecewise-linear (PWL) approximation of a depth-of-discharge-dependent cost, as formulated in (20) [10].

$$C_{deg,t} = \sum_{k=1}^{K} \Delta C_k \left[P_{t,k}^{ch} + P_{t,k}^{dis}\right] \quad (20)$$

where, K is the number of degradation segments and $P_{t,k}^{ch}$ and $P_{t,k}^{dis}$ are segment allocations. ΔC_k is the PWL degradation slope for segment k [JPY/MWh], which is function of the degradation cost coefficient β [11] and depth-of-discharge increment δ, as described in (21).

$$\Delta C_k = \beta \delta^{2.03} \quad (21)$$

F. Decision Variables

Consequently, the optimization simultaneously determines the electrical dispatch, thermal operation, degradation allocation, and FCR market participation of the BESS through the following set of decision variables:

$$X = \begin{Bmatrix} P_t^{ch}, P_t^{dis}, P_t^{exp}, E_t, T_t^b, P_t^{cool}, P_t^{heat}, \\ Q_{b(t)}, n_b, U_t^{ch}, U_t^{dis}, y_b, P_{t,k}^{ch}, P_{t,k}^{dis} \end{Bmatrix}$$

IV. Simulation Data, Parameters, and Scenarios

Herein, the proposed MILP framework is evaluated using real market, load, and environmental data over a continuous six-month horizon (July-December 2024). Furthermore, electricity prices are taken from the JEPX for the Kyushu area [12]. Moreover, realistic purchase prices include wheeling charge (1.27 JPY/kWh), renewable energy surcharge (3.98 JPY/kWh), and non-fossil certificate price (0.40 JPY/kWh). Besides, export revenues are computed by subtracting the generation wheeling charge (0.43 JPY/kWh) from the spot price. On other hand, FCR capacity revenues are applied on a 3-h block basis, consistent with the prevailing market settlement rules during the study period [13].

The 5.5 GWh aggregated EV charging demand is derived from real charging-session data from municipal parking facilities in New York City [14]. However, it is converted into a 30-min average power profile applied as an exogenous load served by the BESS. Additionally, ambient temperature data are obtained from measured observations in Fukuoka [15] and converted to 30-min resolution. Such real logs preserve seasonal thermal variability that influences battery temperature and HVAC operation. All main simulation parameters are summarized in TABLE I and follow prior studies [9], [10], [16].

To isolate the impacts of energy export and FCR participation, four scenarios are evaluated: S1 (EXPoff-FCRoff) considers spot-market charging only, S2 (EXPoff-FCRon) enables reserve provision without export, S3 (EXPon-FCRoff) allows energy arbitrage via export only, and S4 (EXPon-FCRon) combines export with FCR participation. All optimization scenarios are formulated and solved in MATLAB R2024b using the intlinprog MILP solver.

TABLE I. KEY PARAMETERS USED IN SIMULATIONS

Parameter	Description	Value	[unit]
P_{rated}	Rated charge/discharge power	50	[MW]
E_{min}-E_{max}	SoC limits	20-180	[MWh]
Q_{min}, Q_{max}	Min and Max FCR bid	1, 50	[MW]
η_{ch}& η_{dis}	Round-trip efficiency	0.95	–
C_{th}	Thermal capacitance	1.2	[MWh/ °C]
UA	Heat transfer coefficient	0.2	[MW/ °C]
P_{max}^{HVC}	HVAC power limit	0.7	[MW]
COP_c, COP_h	HVAC COPs	3.0, 4.0	–
T_{min}-T_{max}	Temperature limits	15-30	[°C]
β	Cycle aging cost coefficient	13755	[JPY/MWh]

V. RESULTS AND DISCUSSIONS

A. *Whole-Period Economic Outcomes*

Fig. 2 reports the aggregated economic outcomes over the July-December 2024 horizon. In the baseline case without export or FCR (S1), the BESS operates at a net cost of 90.3 MJPY, dominated by spot energy purchases, with degradation and HVAC costs contributing a smaller share. Allowing energy export without FCR (S3) lowers the net cost to 68.0 MJPY, reflecting partial recovery through arbitrage. However, the associated increase in degradation and HVAC costs limits the overall benefit.

In contrast, FCR participation fundamentally alters the economic balance. With FCR enabled and export disabled (S2), capacity revenues of 662.9 MJPY outweigh all operating costs, resulting in a net profit of 547.1 MJPY. Moreover, combining export and FCR (S4) yields a comparable profit of 550.1 MJPY. This modest improvement arises since export partially offsets spot energy costs while leaving degradation and HVAC burdens essentially unchanged.

B. *Daily Economic Trends*

Furthermore, the daily cost, revenue, penalty, and net outcomes for the four scenarios over July-December, indicate clear performance differences. Without FCR participation, revenues are negligible and the net outcome remains near break-even, with average values of approximately +0.5 MJPY/day (S1) and +0.4 MJPY/day (S3) and limited variability (σ ≈ 0.5-1.0 MJPY/day). With FCR enabled, average daily revenue increases to about 3.6 MJPY/day, resulting in consistent net profits of roughly −3.0 MJPY/day. Variability rises modestly (σ ≈ 1.1 MJPY/day), driven mainly by FCR price fluctuations, while no penalties are incurred.

C. *Daily SoC Trends*

Daily SoC trajectories highlight the contrasting operational roles of export-driven arbitrage and FCR-oriented reserve provision, as shown in Figs. 3(a) and (b). In Fig. 3(a), export participation without FCR (S3) induces the most aggressive cycling, with nearly double the charge/discharge throughput relative to non-export operation. Hence, it introduces the largest daily SoC swings (mean ≈ 76 MWh) and frequent excursions toward the energy limits.

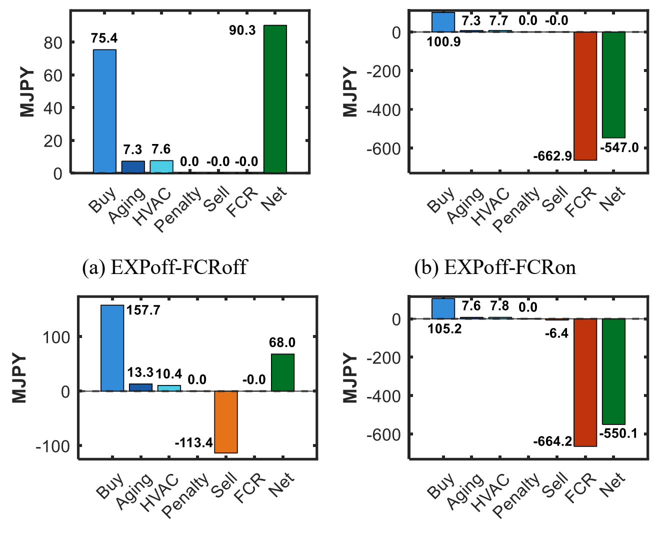

(a) EXPoff-FCRoff (b) EXPoff-FCRon

(c) EXPon-FCRoff (d) EXPon-FCRon

Fig. 2. Operational cost breakdown of the BESS

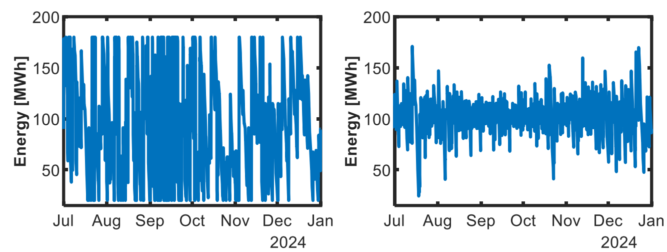

(a) EXPon-FCRoff (b) EXPon-FCRon

Fig. 3. Daily SoC behaviors

In contrast, Fig. 3(b) illustrates how FCR participation (S4) fundamentally reshapes SoC behavior. Specifically, the operation is concentrated around mid-range levels (≈ 100-103 MWh), daily swings are reduced to about 35 MWh, and extreme excursions (ΔSoC ≥ 120 MWh) are eliminated. Moreover, FCR operation raises the minimum SoC by approximately 4-6 MWh, preserving reserve headroom and avoiding deep depletion.

D. *Daily Thermal Trends*

To capture the dominant thermal behavior, Figs. 4(a) and (b) present representative temperature profiles for S3 and S4. In both cases, the thermal controller strictly enforces the hard limits, keeping the battery temperature within 15-30 °C for the entire six-month horizon. The mean operating temperature remains tightly clustered at ≈23.7-23.8 °C, indicating stable thermal regulation.

Export-only operation induces deeper cycling and significantly higher cooling demand. However, it does not widen the temperature range, as the additional thermal stress is handled through increased HVAC activity. In contrast, FCR participation maintains similar temperature stability with lower cooling effort, highlighting the moderating effect of reserve-oriented dispatch.

Moreover, Fig. 5 compares the cooling and heating electricity demand of the BESS thermal management system across the four scenarios. In S1, S2, and S4, heating slightly dominates the HVAC electricity consumption, accounting for about 52-53% of the total, while cooling represents 47-48%. In contrast, S3 shows a noticeably higher HVAC demand (578.9 MWh), where cooling becomes dominant (59.1%), reflecting the increased thermal load during export-driven operation.

E. Assessment I Compliance

Herein, the distribution of offered FCR capacity for EXPon-FCRon (S4) is illustrated. According to Fig. 6, the bidding profile is concentrated between approximately 21-27 MW, with a mean (median) value of 22.52 MW (24.15 MW) and a maximum of 26.63 MW. Moreover, the 25^{th}-75^{th} percentile range spans from 20.93 MW to 26.02 MW, indicating consistently high reserve provision. Over the full horizon, the BESS delivers 199430.6 MWh of reserve capacity under strict Assessment I compliance.

F. Daily Degradation Trends

Daily degradation cost strongly depends on the operating strategy, as shown in Fig. 2. Export-only operation (S3) results in the highest degradation, reaching 13.28 MJPY over the study period. This increase is caused by deeper and more frequent cycling driven by spot-market arbitrage.

With FCR participation, degradation remains effectively constrained. Total aging cost stays close to the non-export baseline at 7.3-7.6 MJPY (≈0.040-0.042 MJPY/day), even when export is enabled. Consequently, the degradation share of energy-related costs decreases from 24.3% in S3 to approximately 6.7-7.2% in FCR cases. This limited impact reflects the Assessment I-only modeling. Practically, Assessment II activation would increase droop-driven cycling and degradation.

VI. CONCLUSION

This work introduces a market-consistent MILP model for large-scale BESS participation in Japan's FCR market. Specificity, the model includes thermal dynamics, degradation, and auxiliary power consumption using real market data. Particularly, results show that energy export alone provides limited benefit. Moreover, although spot energy costs decrease by ≈41%, degradation and HVAC costs increase by ≈82% and ≈37%, respectively, resulting in only a ≈25% reduction in net cost. In contrast, FCR participation revenues exceeding 660 MJPY convert BESS operation from a net cost to a net profit of about 550 MJPY.

Operationally, reserve-oriented dispatches reduce daily SoC swings by ≈54%, raises minimum SoC by 4-6%, and eliminates extreme excursions. Furthermore, the degradation share of energy-related costs drops from 24.3% to below 7.2%. Finally, thermal limits are satisfied for 100% of the horizon, confirming feasibility under sustained high utilization.

Future work will incorporate Assessment II dynamic activation based on droop control, including slot-level bidding and pricing under Japan's updated FCR rules effective from April 2026.

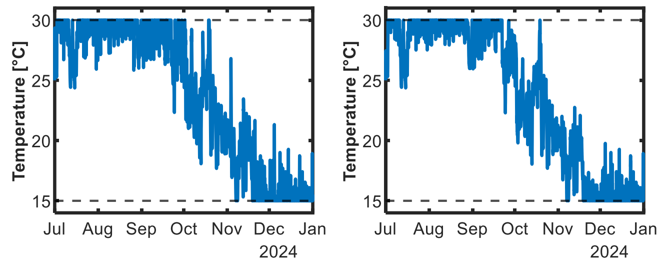

(a) EXPon-FCRoff (b) EXPon-FCRon

Fig. 4. Daily BESS's temperature behaviors

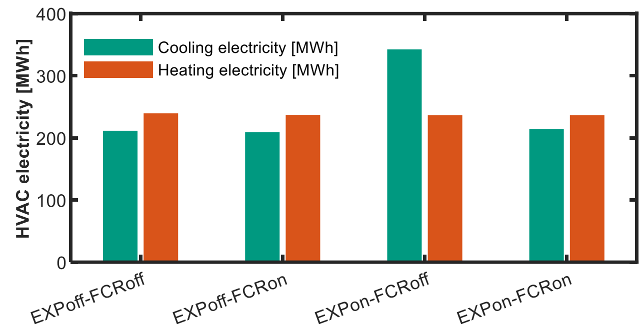

Fig. 5. Cooling and heating electricity demand

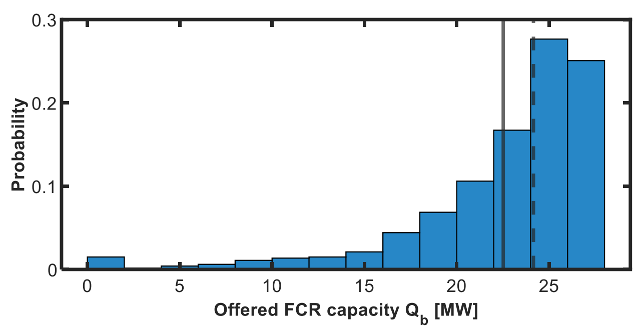

Fig. 6. Histogram of offered FCR capacity for EXPon-FCRon

ACKNOWLEDGMENT

This work is conducted by the Social Cooperation Research Departments of Power System Innovation Realization with Fuji Electric Co., Ltd. in Collaborative Research Organization for Comprehensive Energy Sciences (CROCES) at The University of Tokyo.

REFERENCES

[1] A. Yokoyama, "Toward deregulated, smart and resilient power systems with massive integration of renewable energy in Japan," IEEJ Trans. Electr. Electron. Eng., vol. 17, no. 9, pp. 1242–1254, Sep. 2022.

[2] M. Nakamura and S. Tamura, "Preliminary study of economic evaluation of electric power supply for university campus equipped with heat/cool storage facilities using JEPX and BESS control," in Proc. 2018 IEEE Int. Telecommun. Energy Conf. (INTELEC), pp. 1–6, Oct. 2018.

[3] M. Mae, R. Matsuhashi, K. Nakamura, and H. Bessho, "Model predictive control for imbalance compensation of solar power generation in local area energy management system," in Proc. 21st Int. Conf. Eur. Energy Market (EEM), pp. 1–6, May 2025.
[4] M. Matsubara, M. Mae, and R. Matsuhashi, "Pilot study on residential measures against unpredictable outages with batteries and photovoltaics considering necessary loads," in Proc. 20th Int. Conf. Eur. Energy Market (EEM), pp. 1–6, Jun. 2024.
[5] Renewable Energy Institute, "Unlocking the potential of grid-scale battery storage business: Current status and challenges," Aug. 2025. [Online]. Available: https://www.renewable-ei.org/en/activities/reports/20250807.php. Accessed: Feb. 10, 2026.
[6] M. Ahouad, A. Sunjaq, E. Wikner, and T. Thiringer, "Economic assessment of battery energy storage for frequency regulation in the Nordic power systems," in Proc. 20th Int. Conf. Eur. Energy Market (EEM), pp. 1–5, Jun. 2024.
[7] A. Mohamed, R. Rigo-Mariani, and V. Debusschere, "Impact of modeling assumptions on the economic performance assessment of a storage participating in energy and reserve markets," J. Energy Storage, vol. 133, pp. 117998, Oct. 2025.
[8] U. Mumtahina, S. Alahakoon, and P. Wolfs, "A day-ahead optimal battery scheduling considering the grid stability of distribution feeders," Energies, vol. 18, no. 5, p. 1067, Feb. 2025.
[9] I. Rajah, J. Sowe, M. Schimpe, and J. V. Barreras, "Degradation-aware derating of lithium-ion battery energy storage systems in the UK power market," Electronics, vol. 13, no. 19, p. 3817, Sep. 2024.
[10] R. Khalilisenobari and M. Wu, "Optimal participation of price-maker battery energy storage systems in energy and ancillary services markets considering degradation cost," Int. J. Electr. Power Energy Syst., vol. 138, pp. 107924, Jun. 2022.
[11] Ministry of Economy, Trade and Industry (METI), "Energy audit under the initiative on distributed energy system for Phayam Island: Final report," FY2022. [Online]. Available: https://www.meti.go.jp/meti_lib/report/2022FY/000534.pdf. Accessed: Feb. 10, 2026.
[12] Japan Electric Power Exchange (JEPX), "Electric power market data (spot market)." [Online]. Available: https://www.jepx.jp/en/electricpower/market-data/spot/. Accessed: Feb. 10, 2026.
[13] Electrical Power Reserve Exchange (EPRX), "Reserve market results." [Online]. Available: https://www.eprx.or.jp/information/results.php. Accessed: Feb. 10, 2026.
[14] U.S. Department of Transportation, "Electric vehicle (EV) charging data—municipal lots and garages." [Online]. Available: https://catalog.data.gov/dataset/electric-vehicle-ev-charging-data-municipal-lots-and-garages. Accessed: Feb. 10, 2026.
[15] Japan Meteorological Agency (JMA), "Meteorological data." [Online]. Available: https://www.jma.go.jp/jma/indexe.html. Accessed: Feb. 10, 2026.
[16] N. Ketjoy, W. Chamsa-ard, T. Suriwong, Y. Mensin, U. Prasatsap, S. Kumar, S. K. Sahoo, and C. Chantarapongphan, "Technical viability of 136 MWh PV–biogas–battery energy storage power plant: Policy guidelines for BESS-based VRE integration deployment in Thailand," J. Energy Storage, vol. 114, pp. 115851, Apr. 2025.